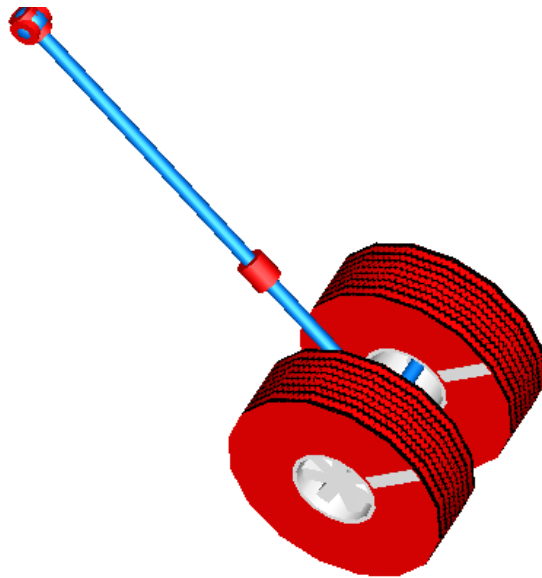




CHALMERS
UNIVERSITY OF TECHNOLOGY



Dynamic modeling and control strategies for shimmy in aircraft landing gears

Master's thesis in System Control and Mechatronics

Tonghui Zhang

MASTER'S THESIS 2016:NN

**Dynamic modeling and control strategies for
shimmy in aircraft landing gears**

Tonghui Zhang



CHALMERS
UNIVERSITY OF TECHNOLOGY

Department of Signals and Systems
CHALMERS UNIVERSITY OF TECHNOLOGY
Gothenburg, Sweden 2015

Dynamic modeling and control strategies for shimmy in aircraft landing gears Tonghui Zhang

© Tonghui Zhang, 2016.

Supervisor: Balázs Adam Kulcsár, Chalmers University of Technology
Jim Claesson, Modelon AB

Examiner: Balázs Adam Kulcsár, Chalmers University of Technology

Master's Thesis 2016:NN
Department of Signals and Systems
Chalmers University of Technology
SE-412 96 Gothenburg
Telephone +46 31 772 1000

Cover:3-D nose landing gear model built in Dymola

Printed by Chalmers Publication Library
Gothenburg, Sweden 2016

Dynamic modeling and control strategies for shimmy in aircraft landing gears
Tonghui Zhang
Department of Signals and Systems
Chalmers University of Technology

Abstract

Air traffic is one of the most important means of transportation methods. It is of importance to make it a safe, efficient, and comfortable experience. Oscillations occurring during landing and taking off at nose landing gear, known as shimmy, may result in gear fatigue, severe failures, or in extreme case accidents.

Engineers never stop trying to analyze and eliminate it by means of nose landing gear shimmy control. Currently, a general method to avoid shimmy is to install a damping component at the torsion link joint as a passive element but still a deeper understanding of shimmy is essential for the design of controller with more accurate and quick responding characters (e.g. electrohydraulic actuators). In contrast to real landing gear tests which are expensive and difficult to perform, a virtual physical model is more economical and easier for dynamic analysis and controller design. Modelon AB, as an expert and market leader on model-based-design systems, known as MBD, has a project on shimmy dynamics and active control. As part of this project, in this thesis, a physical model is created in Dymola based on existing model libraries developed by Modelon AB and a control strategy is proposed to annihilate shimmy oscillation. A traditional math model acts as basics and a model with MF-Swift model (included in the MF-Tyre/MF-Swift product developed by TASS International) is constructed as a contrast experiment. After model linearisation, in Matlab, shimmy controllers are synthesised, such as Linear Quadratic Regulator(LQR), Proportional Integrating Differential(PID) controllers. These controllers will be compared in closed loop scenarios. The model and controller are verified in Dymola.

Keywords: Shimmy, Tyre, LQR, PID, Modelica, Dymola, Matlab

Acknowledgements

This thesis is conducted as part of Master Program System Control and Mechatronics in Chalmers University of Technology in Gothenburg. The thesis is supported by Modelon AB and finished in their Gothenburg office. The scientific data of MF-Swift specified in this thesis belongs to TASS International.

I would like to thank Modelon AB for giving me the chance to work on this thesis and all their employees for their help for me. Especially, I would thank Assistant Prof Balázs Adam Kulcsár for his supervising and Jim Claesson for our discussions on my thesis.

Tonghui Zhang, Gothenburg, September 2016

Notations

symbol	Description
a	Slip angle
$a_{1,2,3,\dots}$	Coefficient of the character equation
c	Torsional spring rate
$c_{f\alpha}$	Side force derivative
$c_{m\alpha}$	Moment derivative
e	Caster length
ϵ	Error between the reference and the output
$f(x, u)$	Mapping function $\mathbb{R}^n \times \mathbb{R}^m \rightarrow \mathbb{R}^n$
k	Torsional link damping constant
k_p	Proportional gain
$q_{1,2,\dots,n}$	State design parameters for Bryson rule
$r_{1,2,\dots,m}$	Input design parameters for Bryson rule
s	Laplace variable
t	Time
t_e	Time at the equilibrium point
t_0	Initial time
u	Input signal to the system
\bar{u}	Input signal at the equilibrium
$u_{1max,2max,\dots,mimx}$	Input limitations
\tilde{u}	Input signal of the simplified system
x	State vector of the system
$x_{1,2,\dots}$	Element of the state vector
\bar{x}	States at the equilibrium point
$x_{1max,2max,\dots,nimx}$	States limitations
\tilde{x}	States of the simplified system
y	Measured outputs
y_c	Lateral shift of the tyre center
y_l	Lateral shift of the leading contact point
\tilde{y}	Measured outputs of the simplified system
A	State matrix of the system
\tilde{A}	State matrix of the simplified system
B	Input matrix of the system
\tilde{B}	Input matrix of the simplified system
C	Output matrix of the system
\tilde{C}	Output matrix of the simplified system
C^{-1}	Inverse transformation of the output matrix
F_x	Longitudinal force of the tyre
F_y	Lateral force of the tyre
F_z	Vertical load force
I_z	Vertical inertia
J	Cost function
K	Feedback gain

L	Lagrange formula
M_x	Longitudinal moment
M_y	Lateral moment
M_z	Self aligning torque
M_1	Spring moment
M_2	Damping moment
M_3	Total tyre moment around z-axis
M_4	Tread width damping moment
O	Controllability matrix
P	Riccati differential equation matrix
Q	States weight matrix
R	Input weight matrix
T_d	Derivative time
T_i	Integral time
V	Taxiing velocity
W	Observability matrix
α	Slip angle
α_g	Slip angle limitation of the tyre moment
δ	Small variation
δ_x	Small variation of state x
δ_u	Small variation of input u
ϵ	Error between the output and the reference
ε	A small variable
ζ	Slip angle limitation of the tyre force
κ	Tread width moment constant
λ	Co-state of Euler Lagrange equation
σ	Relaxation length of the tyre
ϕ	Rake angle of the landing gear
ψ	Yaw angle
$\Gamma, \Theta, \Lambda, \Upsilon$	Magic formula coefficients
Ω	Torque or force of a tyre
τ	Transpose of a matrix or a vector
$*$	Optimal of a variable

List of Figures

1.1	Schematic overview of different landing gear configurations[1]	2
1.2	Feedback diagram	3
2.1	Top view of shimmy dynamics model[9]	5
2.2	Nonlinear $\frac{F_y}{F_z}$ vs slip angle[10]	7
2.3	Nonlinear $\frac{M_z}{F_z}$ vs slip angle[10]	7
2.4	Straight tangent tyre model (top view)[1]	8
2.5	Stability velocity zone with different damping constant	10
2.6	Eigenvalue curves in a range of velocity	10
2.7	Yaw angle shimmy responds to a pulse disturbance	11
2.8	Frequency analysis of shimmy responds	11
3.1	Mechanical Structure	13
3.2	Linear Tyre Model	14
3.3	Hydraulic supplying unit	15
3.4	Hydraulic supplying unit	16
3.5	Test rig	17
4.1	MF-Swift model simulation	19
4.2	Linear tyre simulation	20
4.3	Complete Simulation result	20
4.4	Zeros and poles of system	21
4.5	Bode diagram	23
5.1	Yaw angle using PI, PD, PID controllers	26
5.2	Bode graph of uncontrolled system, PID controlled system and PID controlled system with low-pass filter	26
5.3	Simulation results with different Q	28
5.4	PID and LQR simulation comparison	29
5.5	Bode graph of Open-loop, LQR controlled and PID controlled system	29

Contents

Abstract	v
Acknowledgements	vii
Notations	ix
List of Figures	xi
1 Introduction	1
1.1 Background	1
1.2 Problem Statement	1
1.3 Thesis Scope	1
1.4 Landing Gear Structure	2
1.5 Feedback Control	3
1.6 Linear Quadratic Regulator	3
1.7 MF-Swift Model	3
1.8 Tools	4
2 Theory	5
2.1 Mathematical Model	5
2.2 Jacobian Linearization	9
2.3 Analysis	10
2.4 Simulation	11
3 Method	13
3.1 Mechanical System Modeling	13
3.2 Tyre Modeling	14
3.3 Hydraulic System Modeling	15
3.4 Test Rig Modeling	16
3.5 Parametrization	17
4 System Analysis	19
4.1 Simulation	19
4.2 System Analysis	21
4.2.1 Stability	21
4.2.2 Controllability and Observability	22
4.3 Simplification	22

5	Controller Design	25
5.1	PID Control	25
5.2	LQR Design	27
5.3	Controller Analysis	28
6	Conclusion and Discussion	31
6.1	Conclusion	31
6.2	Limitations	31
6.3	Future Work	31
	Bibliography	33

1

Introduction

This report develops a model of shimmy phenomenon on nose landing gear in Dymola and control algorithm design for it. The thesis is supported by Modelon AB and will be used for future products in Dymola.

1.1 Background

Shimmy is the self-induced vibration in a frequency range of 10 to $30Hz$ caused by the tyre lateral dynamic mechanism and landing gear structure occurring on both nose and main landing gears. Sometimes it might result in severe failures even accidents in extreme cases [1]. Shimmy dynamics have been studied for a long history. In 1925, French engineer, Broulhiet observed that tyre dynamic performance was an essential factor contributing shimmy which is still of significance in shimmy analysis and control. Different from Broulhiet's method, another French engineer Sensaud de Lavaud concentrated on a rigid tyre model disregarding ground force effects. In 1950, hardware component like shimmy damper began to be installed at the torsion link on landing gears but still, not enough understanding of shimmy was available. In 1951, a program involving shimmy theory, computer aided study, experimental study and a full scale of testing was started in Wright Air Development Center. In 1954, Fromm investigated the relationship between lateral forces and yaw angle or slip. In 1970s, many researches attributed that shimmy is due to tyre imperfections or abrasion and road surface roughness. By now, gear designers realized that to fully understand shimmy phenomenon, it was necessary to account plane flexibility, tyre dynamics, landing gear structure and components together [2].

1.2 Problem Statement

Most existed shimmy explorations are based on mathematical model which are not enough sufficient to reflect the real performance. Therefore, a thorough landing gear model together with the hydraulic system is necessary for virtual experiments and a shimmy control algorithm could be designed based on it.

1.3 Thesis Scope

This thesis includes 3 main tasks

- Creating a 3-D landing gear model including the hydraulic system to expose shimmy phenomenon.
- Design a control algorithm to eliminate shimmy.
- Building a test rig to compare the open loop and controlled system.

To build a reasonable physical model, a traditional math model is stated as the theoretical basement and a complete tyre model developed by TASS International works as a comparison. In chapter 5, a linear quadratic regulator and a PID controller are analyzed and compared for a better performance.

1.4 Landing Gear Structure

Landing gear is one of the most critical components laid under the aircraft fuselage for smooth landing. In reference [3], a 35-year period research shows totally 456 aircraft accidents related to landing gears ranking number one in all accident factors. Therefore, optimizing the structure and components of the landing gear is still of importance. A number of landing gear prototypes are shown in figure 1.1.

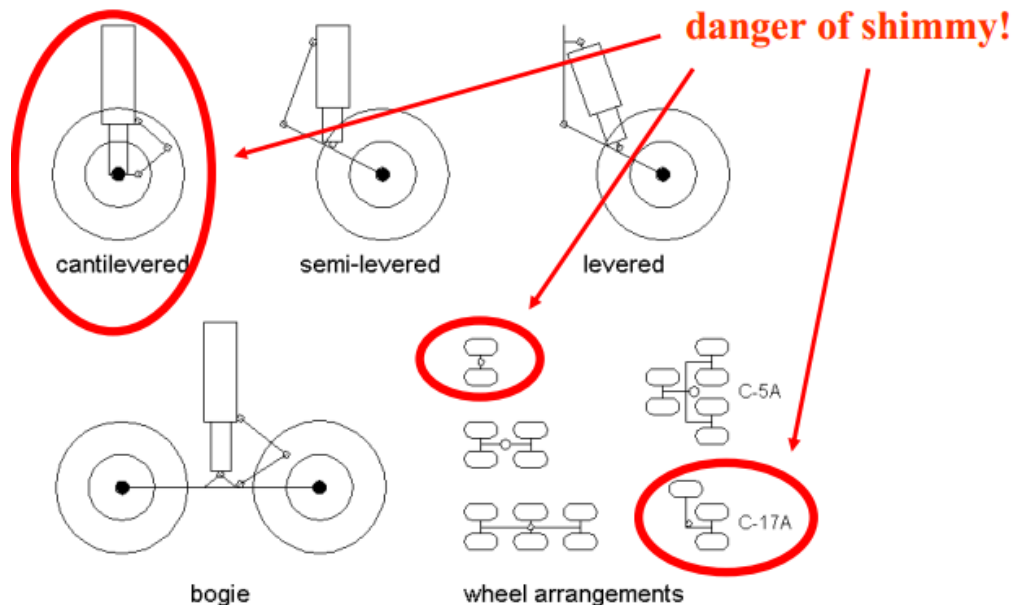


Figure 1.1: Schematic overview of different landing gear configurations[1]

For modern civic airplanes, the twined cantilevered style is the most popular structure for nose landing gear by far. In this thesis, the cantilevered twin-wheel structure is adjusted with a rake angle.

1.5 Feedback Control

In the field of industrial engineering, a control system is a system consisting of a range of elements affected by each other dynamically with desired commands to the system as inputs and specified system responds as outputs. Usually, systems are defined in two categories: open-loop and closed-loop. The open-loop system is not contributed by its outputs while in contrast, a closed-loop system or feedback system dynamic behaviour is dependent on both desired inputs, known as set points, and measured outputs [4]. A feedback system block diagram is in the style of figure 1.2.

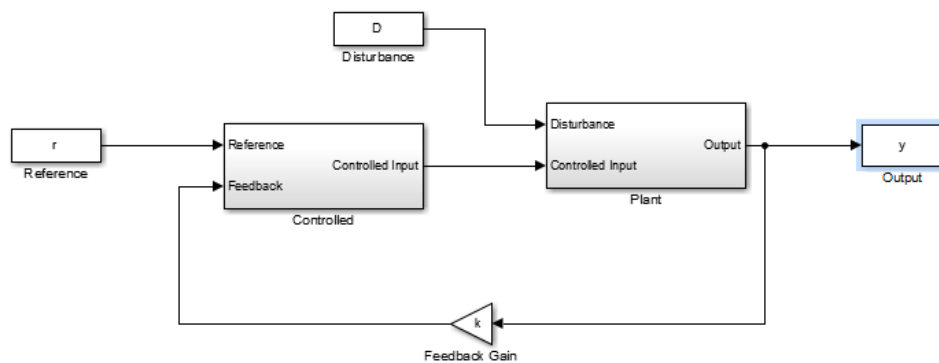


Figure 1.2: Feedback diagram

There are two types of feedback systems, positive and negative. The positive feedback works like an amplifier increasing the effect of the input while the negative feedback is an error regulator minimizing the difference between the reference signal and the output. The selection of positive or negative feedback is based on the requirements and for most stabilization target, usually negative feedback is more suitable [5].

1.6 Linear Quadratic Regulator

A control target on a linear system with a cost function respect to states and inputs is called Linear Quadratic problem and a solution to minimize or maximize the cost function is called Linear Quadratic Regulator. Parameters of the cost function are selected by engineers depending on the cost of input energy and output accuracy. The cost function could either use all states as a state feedback control problem or choose specified states as output optimal control [6]. A description of the algorithm in detail is included in chapter 5.

1.7 MF-Swift Model

An important factor which affects the shimmy phenomenon is the contact effort between tyres and road. Traditionally, engineers usually optimize the road condition

so that automobiles have comfortable and safe operating performance. To make vehicle dynamic properties accurate, TASS International provides a complete chain of modeling and detailed assessment of tyre-road interaction [7]. In this thesis, the MF-Swift model with latest implementation of renowned 'Magic Formula' is used to present performance of a suitable frequency.

The 'Magic Formula' is developed by Pacejka to describe tyre dynamic characters. over the last decades, 'magic formula' has been applied on a series tyre modeling design and analysis. Despite there are no particular theoretical physical foundations for tyre dynamic equations even though they fit a wide range of tyre conditions, 'Magic Formula' is widely used for automobile modeling and landing gear tyre modeling with a general expression as shown in 1.1,

$$\Omega(\alpha) = \Gamma \sin(\Lambda \arctan(\Theta(1 - \Upsilon)\alpha) + \Upsilon \arctan(\Theta\alpha)) \quad (1.1)$$

The tyre forces and torques $R(\alpha)$ are calculated with respect to slip angle α , vertical force F_z and tyre property parameters Θ , Λ , Γ and Υ . The 'Magic Formula' has benefits that it is easy to program and reasonably accurate even though not work for low speed model [11].

According to [7], MF Swift model is developed based on the MF-Tyre model which enables fast and robust tyre-road force and moment referred to 'Magic formula' for steady-state and transient tyre behavior simulation. Contact forces F_x, F_y and moments M_x, M_y, M_z are calculated using longitudinal, lateral and turn slip and wheel inclination angle with vertical angle as input signal.

Different from MF-Tyre model, MF-Swift model is a rigid ring model and it has been validated to be accurate in the vibration experiments in velocity between $7m/s$ to $40m/s$ up to $100Hz$. It has 5 operation modes for tyre model in which the Rigid ring dynamics with initial statics mode is used for shimmy under $100Hz$. In this mode, all contact forces and moments are included together with a turn slip.

Modelon AB has developed an interface library support Deft-Tyre modeling activities. With this interface, the visualization geometry and operation mode could be selected. In this thesis, the interface model with one frame connected to a revolute joint is simple enough to get desired output.

1.8 Tools

Modelica is an object oriented programming language for modeling of multi-domain of complex system. It has two main characters which are different from general programming languages such as Java.

- Modelica is a modeling language which means it is not compatible in the usual sense. Before exercised by a simulation engine, the modelica block should be translated into objects in advanced.
- Even though statements and algorithmic components are contained in modelica, the equation is in the highest priority content.

Modelica is supported by software Dymola used in this thesis and the analysis and controlling design is finished with Matlab.

2

Theory

In literature [8], Brouhiet described that the wheel shimmy phenomenon results from the forward kinetic energy which changes due to taxiing velocity V and self-excitation energy. When an airplane is taxiing, small disturbance laterally outside will trigger this oscillation. Usually, this oscillation will grow up from small amplitude vibration to a magnitude saturated oscillation. Currently, standard method to avoid shimmy is to use different type of dampers on the Nose Landing Gear even though the dynamic of shimmy is less known. In this chapter, a theoretical description will clearly explain how shimmy is generated and the simulation result of it.

2.1 Mathematical Model

For standard landing gear model, it is composed of the main structure including a torsion link which is essential for shimmy and a twin wheel with rigid lateral characters. A classical nonlinear landing gear model is proposed by Gerhard Somieski in [9]. Figure 2.1 is this classical simple landing gear configuration to be analyzed.

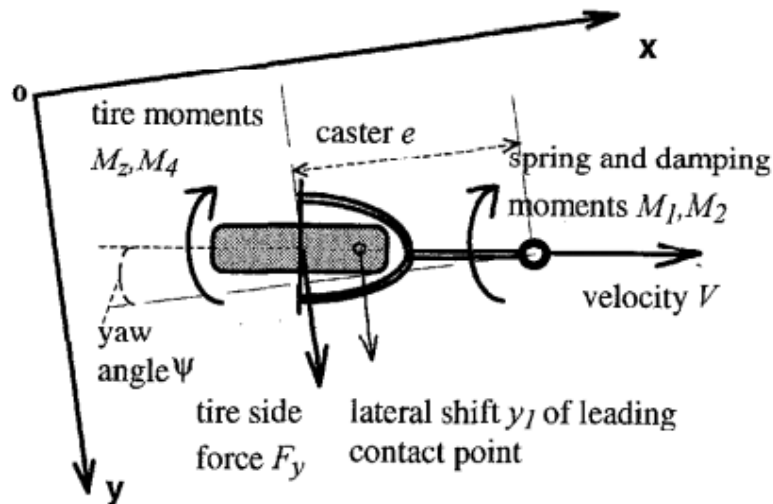


Figure 2.1: Top view of shimmy dynamics model[9]

In figure 2.1, the wheel is mounted on a trailing arm which could rotate around a vertical rotation axis. A linear revolute spring and a damper are added to the

system to simulate the torsion link with the consideration of viscous friction in the oleo strut. The whole structure is mounted under the fuselage of the airplane which is moving with a velocity V .

All necessary parameters for the math model are shown in table 2.1

Table 2.1: Parameters for shimmy

Parameter	Value	Unit
Half contact length a	0.1	m
Caster length e	0.1	0.1
Moment of Inertia I_z	1	kgm^2
Vertical force F_z	9000	N
Torsional spring rate c	-10000	Nm
Side force derivative $c_{f\alpha}$	20	$1/rad$
Moment derivative $c_{m\alpha}$	-2	m/rad
Torsional damping constant k	0 to -50	$Nm/rad/s$
Tread width moment constant κ	-270	Nm^2/rad
Relaxation length σ	0.3	m
Limit angle of tyre moment α_g	10	$degree$
Limit angle of tyre force ζ	5	$degree$

For the whole system, the vertical torque relation could be modeled as a second order system shown in 2.1,

$$I_z \ddot{\psi} = M_1 + M_2 + M_3 + M_4 \quad (2.1)$$

Moments $M_1 = c\psi$ and $M_2 = k\dot{\psi}$ are the torques provided by the torsion link and the effect of the viscous friction in the bearing of the oil-pneumatic shock absorber. M_3 is a tyre moment composed of its own self-aligning moment and the torque generated by lateral force F_y . M_4 is a tyre damping moment from tyre tread width depending on the taxiing velocity and yaw angle [10].

As described previously, moment M_3 is composed of a self-aligning moment and a torque generated by lateral force.

$$M_3 = M_z - eF_y \quad (2.2)$$

In the equation above, e is the caster length of the landing gear and M_z and F_y could be calculated using related formulas in literature [11]. The nonlinear character is described in equation 2.3 and the curve is shown in 2.2

$$F_y = \begin{cases} c_{f\alpha}\alpha F_z & \text{if } |\alpha| \leq \zeta \\ c_{f\alpha}\alpha_g F_z \text{sign}(\alpha) & \text{if } |\alpha| > \zeta \end{cases} \quad (2.3)$$

Where ζ is a limitation of slip angle and α is the slip angle of the tyre.

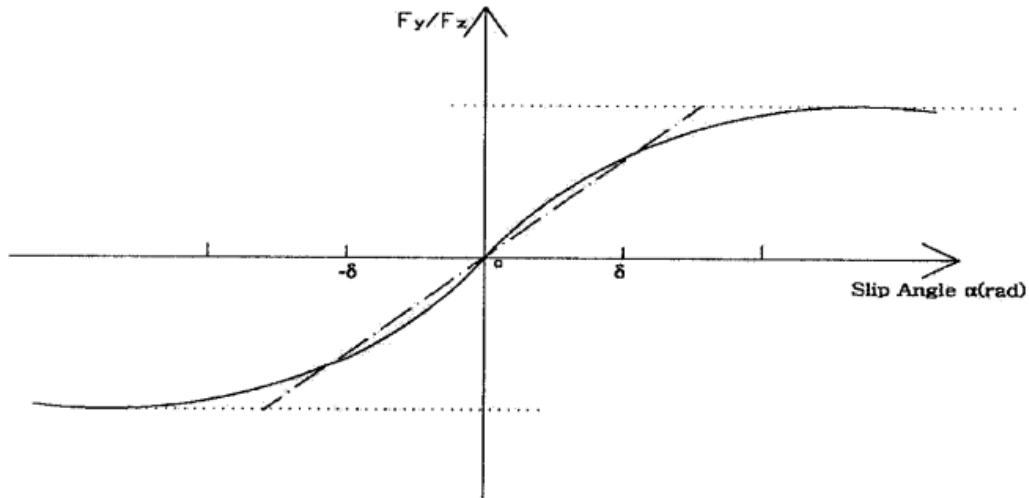


Figure 2.2: Nonlinear $\frac{F_y}{F_z}$ vs slip angle[10]

Another component of M_3 is the self-aligning torque generated when there is a yaw angle on the tyre. In the presence of a non-zero slip angle, this torque tends to turn the wheel to the travelling direction of the landing gear [9]. The value of M_z has a sinusoid expression with respect to the slip angle in the angle limitation zone while 0 outside. The curve and equation are shown below.

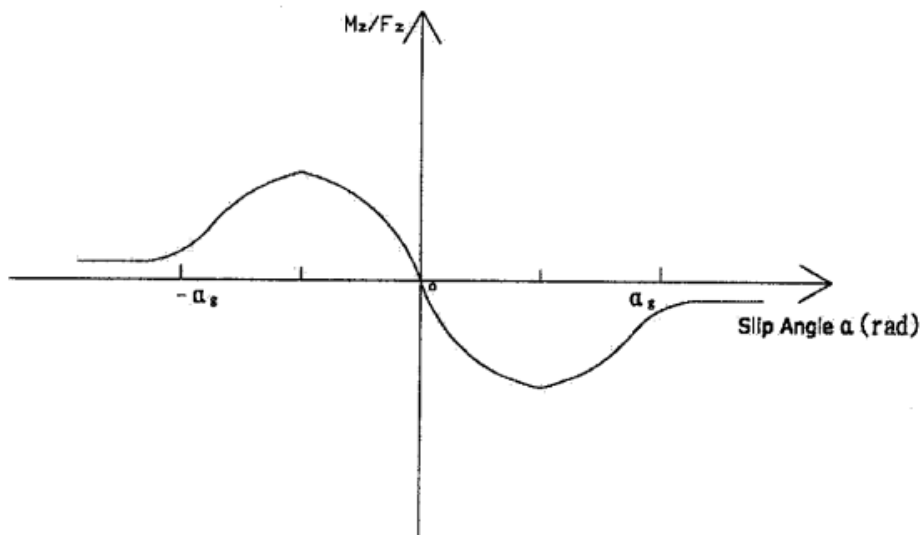


Figure 2.3: Nonlinear $\frac{M_z}{F_z}$ vs slip angle[10]

$$M_z = \begin{cases} F_z(c_{m\alpha} \frac{\alpha_g}{\pi} \sin(\frac{\pi}{\alpha_g}\alpha)) & \text{if } |\alpha| \leq \zeta \\ 0 & \text{if } |\alpha| > \zeta \end{cases} \quad (2.4)$$

M_4 , known as a tyre damping moment, is linear related to the yaw angle velocity of tyre,

$$M_4 = \frac{\kappa}{V} \dot{\psi} \quad (2.5)$$

Where $\kappa = -0.15a^2c_{f\alpha}F_z$.

The detailed analysis and discussion of these moments could be found in literature [9]. the rolling tyre lateral dynamic characters could be described using stretched string theory with a finite contact length introduced by Von Schlippe in 1941. The detailed discussion of stretched string theory could be found in reference [11].

To simplify the problem, a massless tyre model with a string of finite contact length in a circular shape is used to analyze the lateral elastic character. Furthermore, the equilibrium of forces acting on the circular string is somewhat more complicated. Pacejka noted that in the expression for the self-aligning torque derived by Von Schlippe, a corrective factor was introduced, which would not exist if the point of application for all forces acting on the string had been taken into account correctly [11]. The tyre-ground contact model is shown in 2.4.

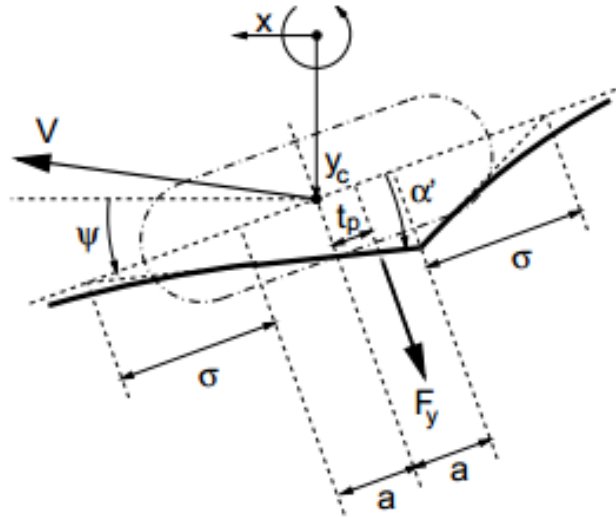


Figure 2.4: Straight tangent tyre model (top view)[1]

The half contact length is a and define y_l as the leading contact point lateral shift, therefore, as what figure 2.4 shows, sliding angle $\alpha \approx \frac{y_l}{\sigma}$ where y_l is the lateral shift of the contact point and σ is the relaxation length. Equation 2.6 could describe the relationship between contact point shift and tyre center lateral shift.

$$\sigma\dot{\alpha} + V\alpha = V\psi - a\dot{\psi} - \dot{y}_c \quad (2.6)$$

$y_c = -e\psi$ could be calculated according to figure2.4 and therefore,

$$\dot{y}_l + \frac{V}{\sigma}y_l = V\psi + (e - a)\dot{\psi} \quad (2.7)$$

The variable yaw angle ψ , yaw angular velocity $\dot{\psi}$ and leading point lateral shift y_l are selected as state variables to formulate a desired standard state space model

with $x_1 = \psi$, $x_2 = \dot{\psi}$ and $x_3 = y_l$.

$$\begin{aligned} \dot{x}_1 &= x_2 \\ \dot{x}_2 &= \frac{c}{I_z}x_1 + \frac{1}{I_z}\left(k + \frac{\kappa}{V}\right)x_2 + \frac{F_z}{I_z}\left(c_{m\alpha}\frac{\alpha_g}{\pi}\sin\left(\frac{\pi}{\alpha_g}\frac{y_l}{\theta}\right) - ec_{f\alpha}\frac{y_l}{\theta}\right)x_3 \\ \dot{x}_3 &= Vx_1 + (e - a)x_2 - \frac{V}{\sigma}x_3 \end{aligned} \quad (2.8)$$

Most control theories consider linear time invariant as objectives and the nonlinear system should be linearized before further analysis.

2.2 Jacobian Linearization

For a nonlinear system

$$\dot{x}(t) = f(x(t), u(t)) \quad (2.9)$$

Where f is a mapping function $\mathbb{R}^n \times \mathbb{R}^m \rightarrow \mathbb{R}^n$. The states vector $x \in \mathbb{R}^n$ is equilibrium if there is a specified input $u \in \mathbb{R}^m$ such that $f(\bar{x}, \bar{u}) = 0$. If $x(t_0) = \bar{x}$ and let $u(t) = \bar{u}$ for any $t > t_0$, the system states will never change to other positions. Define small deviation $\delta_x = x(t) - \bar{x}$, $\delta_u = u(t) - \bar{u}$, the differential equation could be expanded using Taylor expansion method neglecting higher terms as followed.

$$\begin{aligned} \dot{x}(t) &= f(\bar{x} + \delta_x, \bar{u} + \delta_u) \\ &= f(\bar{x}, \bar{u}) + \frac{\partial f(x(t), u(t))}{\partial x} \Big|_{x(t)=\bar{x}, u(t)=\bar{u}} \delta_x + \frac{\partial f(x(t), u(t))}{\partial u} \Big|_{x(t)=\bar{x}, u(t)=\bar{u}} \delta_u \end{aligned} \quad (2.10)$$

$$\begin{aligned} \because x(t) &= f(\bar{x}, \bar{u}) = 0 \\ \therefore \dot{\delta}_x &= \frac{\partial f(x(t), u(t))}{\partial x} \Big|_{x(t)=\bar{x}, u(t)=\bar{u}} \delta_x + \frac{\partial f(x(t), u(t))}{\partial u} \Big|_{x(t)=\bar{x}, u(t)=\bar{u}} \delta_u \end{aligned} \quad (2.11)$$

As long as δ_x and δ_u keep small, the differential equation could be considered as linear time invariant equation,

$$\dot{\delta}_x = A\delta_x + B\delta_u \quad (2.12)$$

where $A = \frac{\partial f(x(t), u(t))}{\partial x} \Big|_{x(t)=\bar{x}, u(t)=\bar{u}}$ and $B = \frac{\partial f(x(t), u(t))}{\partial u} \Big|_{x(t)=\bar{x}, u(t)=\bar{u}}$.

Since the shimmy phenomenon has small variations for all states, the linearized differential equation has similar dynamic characters to the original system when (δ_x, δ_u) is near to (\bar{x}, \bar{u}) . Therefore, the linearized state space model at equilibrium (when $y = 0$) is shown below.

$$\begin{bmatrix} \dot{x}_1 \\ \dot{x}_2 \\ \dot{x}_3 \end{bmatrix} = \begin{bmatrix} 0 & 1 & 0 \\ \frac{c}{I_z} & \frac{1}{I_z}\left(k + \frac{\kappa}{V}\right) & F_z \frac{(c_{m\alpha} - ec_{f\alpha})}{\sigma I_z} \\ V & e - a & -\frac{V}{\sigma} \end{bmatrix} \begin{bmatrix} x_1 \\ x_2 \\ x_3 \end{bmatrix} + \begin{bmatrix} 0 \\ 1 \\ 0 \end{bmatrix} u \quad (2.13)$$

where u is the actuating torque.

2.3 Analysis

The eigen-decomposition for stable analyses is generated as equation 2.14.

$$\lambda^3 - (a_2 + a_5)\lambda^2 + (a_2a_5 - a_1 - a_3a_4)\lambda + a_1a_5 - Va_3 = 0 \quad (2.14)$$

where $a_1 = \frac{c}{I_z}$, $a_2 = \frac{1}{I_z}(k + \frac{\kappa}{V})$, $a_3 = \frac{c_{m\alpha} - c_{f\alpha}}{\sigma I_z F_z}$, $a_4 = e - a$ and $a_5 = -\frac{V}{\sigma}$. In Matlab, it is possible to find the velocity region where the system is stable to avoid disturbances. An important factor which could affect the stability is the damping constant and a comparison of stability of different damping constants with respect to velocity is described in 2.5

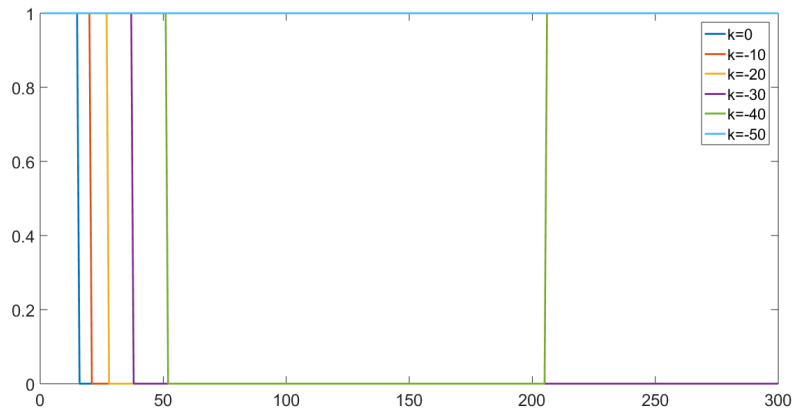


Figure 2.5: Stability velocity zone with different damping constant

Figure 2.5 shows how damping constants affect the stability where 1 indicates stable and 0 means unstable. It is easy to find the stability character with $k = -40$ has a typical curve to describe shimmy with an unstable velocity zone [51 206]. The eigenvalue curve is shown in 2.6.

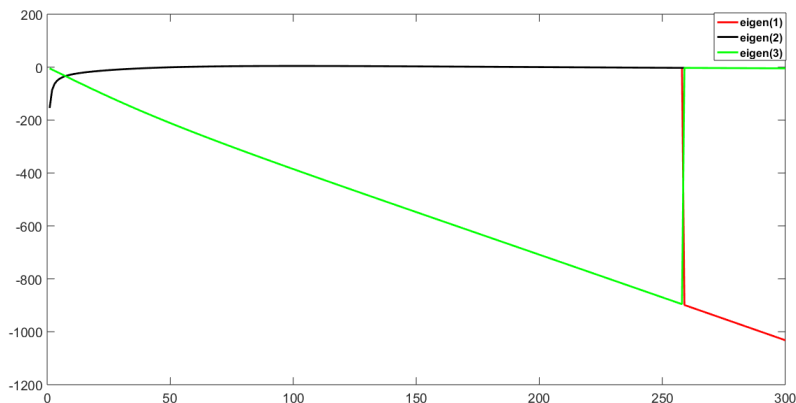


Figure 2.6: Eigenvalue curves in a range of velocity

Therefore, theoretically, the landing gear model will have a shimmy response when the taxiing velocity is between $51m/s$ and $206m/s$.

2.4 Simulation

A math model was built in Dymola and tested using the standard parameters with 3 different taxiing velocities ($50m/s$, $100m/s$, $250m/s$) corresponding to low, mid, high speed. The output is yaw angle and the disturbance is a pulse lateral shift of tyre.

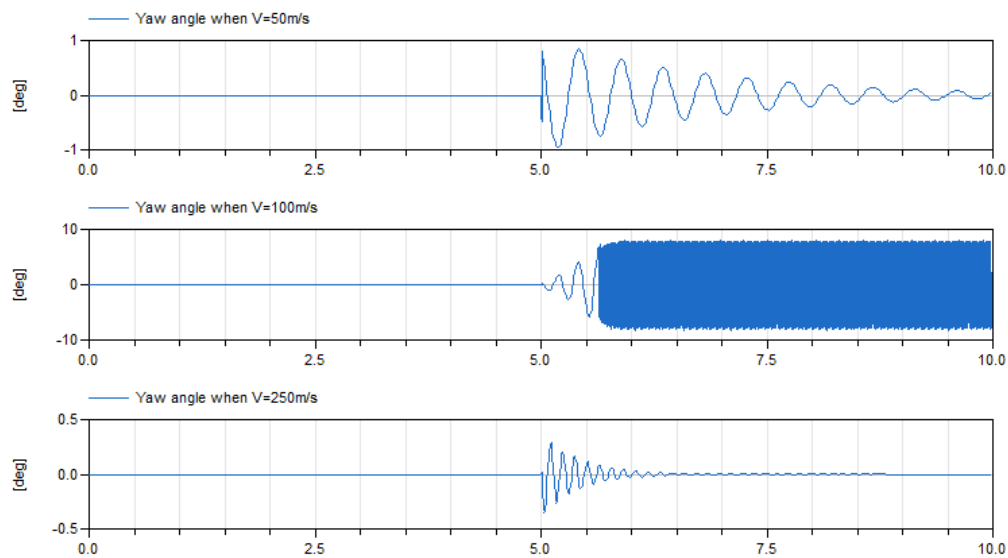


Figure 2.7: Yaw angle shimmy responds to a pulse disturbance

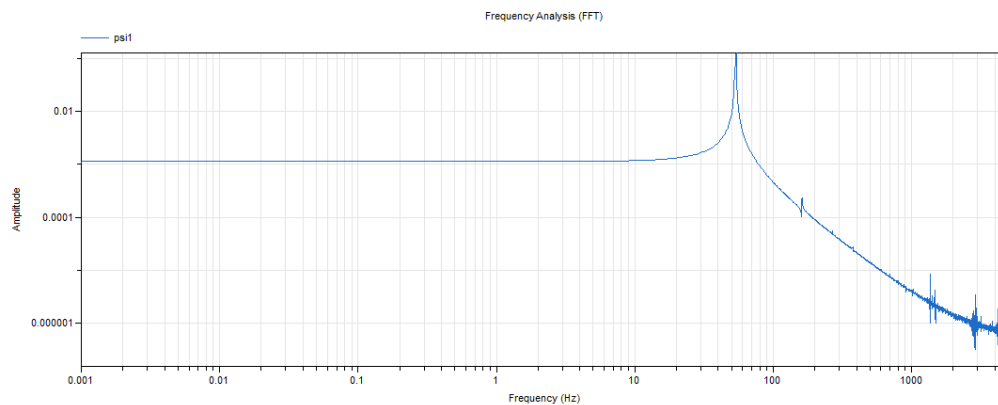


Figure 2.8: Frequency analysis of shimmy responds

Mostly, shimmy frequency is usually in the range of $10 \sim 30Hz$ while for an ideal math model, it could be higher or lower. In Chapter 4, there will be a comparison of different models.

3

Method

For most of the experiments on landing gear dynamic test, it is clear and convenient to analyze simulation results and design control algorithm on a 3D model. Therefore, creating a physical oriented 3D model in Dymola is a good choice. The libraries of mechanical and hydraulic components are supported by Modelon AB and MF-Swift model is supported by TASS International. The parameters are from Airbus manual and empirical value.

3.1 Mechanical System Modeling

The data on the mechanical structure could be found in the AIRBUS manual. In Dymola, the system is built with mechanical library and vehicle library which have more realistic performance. The mechanical diagram with MF-Swift model is shown in figure3.1

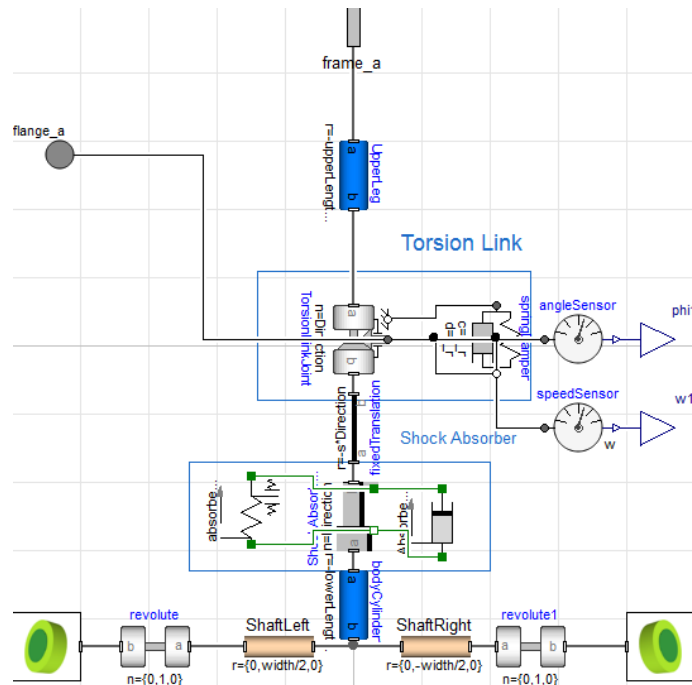


Figure 3.1: Mechanical Structure

The mechanical structure is composed of three main components:

- Oleo pneumatic strut composed of freely rotating upper and lower legs.

3. Method

- Torsional link composed of a vertical revolute joint together with spring-damping component to avoid lower leg's rotating.
- Shock absorber composed of a vertical prismatic joint together with spring-damping component to avoid bouncing up when landing.

Different from the math model, the 3D model does not have the caster link but a rake angle ϕ instead. Also, the shock absorber will affect the taxiing performance when there is a yaw angle in the physical model. A flange connector will be used as the controlled input to the system and two sensors to measure angular velocity and angle as observed outputs.

3.2 Tyre Modeling

A linear tyre model built by Modelon AB is used for analysis and controller design. The block is shown in figure 3.2

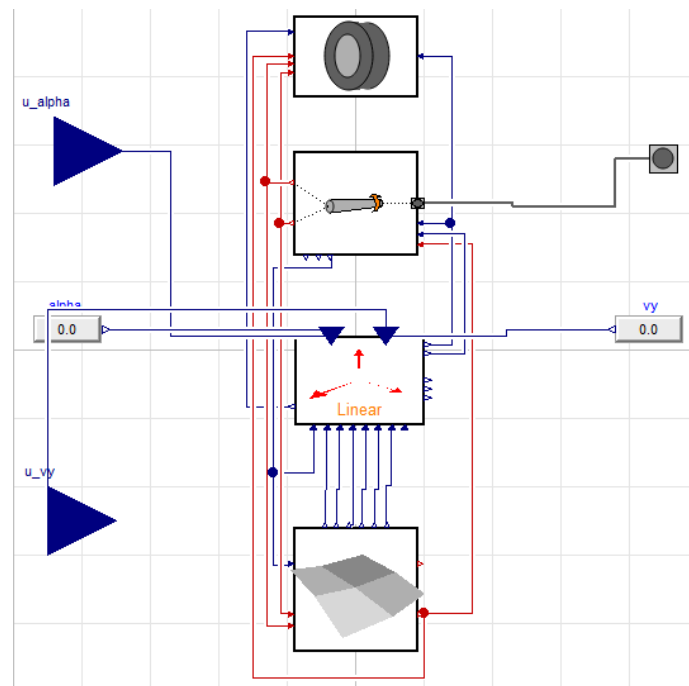


Figure 3.2: Linear Tyre Model

The tyre model is composed of four blocks:

- Rigid (generate the 3-D animation of the tyre model)
- MultiBodyCF (connect the tyre to other components)
- Linear (calculate torques and forces generated by tyres)
- Generic (read forces from the contact of tyre and ground)

To make it corresponding to the math model, a nonlinear self-Aligning torque equation is added in 'linear' block and for disturbance simulation, two variables are added as disturbance sliding angle and lateral shift. The MF-Swift model is used as a comparison experiment with a complete tyre dynamic model.

3.3 Hydraulic System Modeling

The hydraulic system called 'Green system' is composed of three units:

- Hydraulic supplying unit
- Retracting unit
- Steering unit

Since no exact data or geometry is available in this thesis, a component 'Translation to Rotation' is used to transform the linear cylinder force to a rotational torque and two revolute joints to simulate the extension-retraction movement and the steering movement. Figure 3.3 and 3.4 are the block diagrams of supplying unit and retracting unit, the steering unit has a similar structure to the retracting unit.

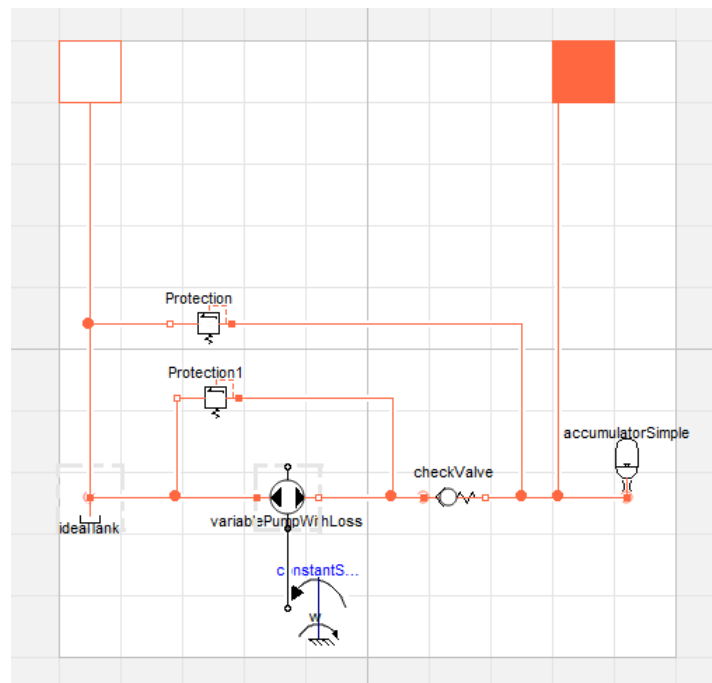


Figure 3.3: Hydraulic supplying unit

As shown in figure 3.3, The hydraulic power is supplied by an ideal constant pump driven by the engine with a constant angular velocity and an ideal tank as a reservoir. A relief valve is installed at the outlet of the pump as a protecting valve and another relief valve to reduce fluids when the system pressure is higher than a standard level. The accumulator is used to reduce fluid fluctuation. A check valve makes the retraction acts in priority compared with than steering action.

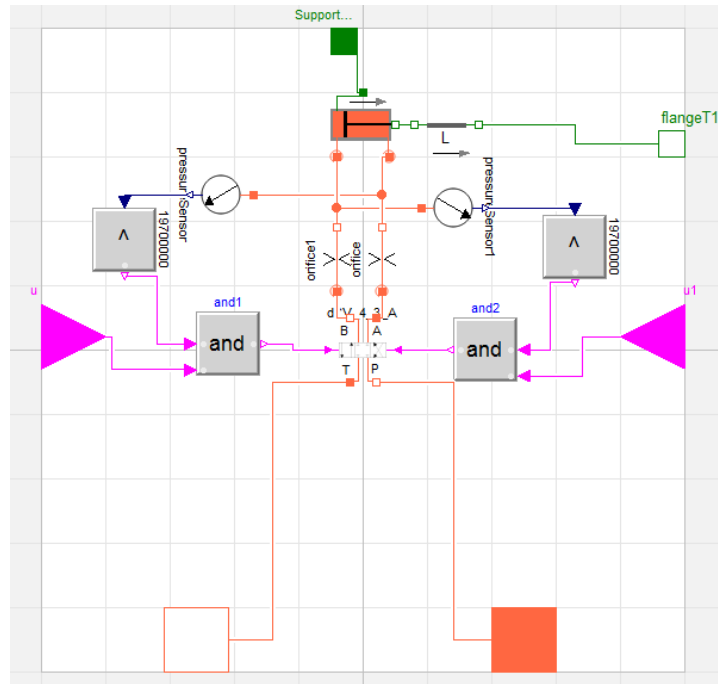


Figure 3.4: Hydraulic supplying unit

The retracting unit is a valve-controlled cylinder system composed of a direction control valve and a differential cylinder in figure 3.4. Two orifices are installed at the inlet and outlet of the cylinder to make the flow to the cylinder at a suitable flow rate and pressure. To make the calculation simpler while protecting the cylinder, two pressure sensors measure the pressure inside and use the feedback signal and input signal to control valve spool position.

3.4 Test Rig Modeling

To test the integrated model, an ideal environment should be built in Dymola. In this thesis, four degrees of freedom are allowed to simulate a taxiing movement:

- Taxiing as a prismatic movement in x axis
- Lateral shift in y axis
- Vertical movement in z axis
- Steering movement around the landing gear axis

A ground component 'flat' is included to give ideal tyre ground contact and another revolute joint with respect to y axis to model the retraction joint. The disturbance used in the experiment is an impulse signal to tyre lateral shift or slip angle. Since the four degrees of freedom belong to the airplane body, a body component is connected to the landing gear with a huge mass and inertia. The whole experiment diagram is shown in figure 3.5

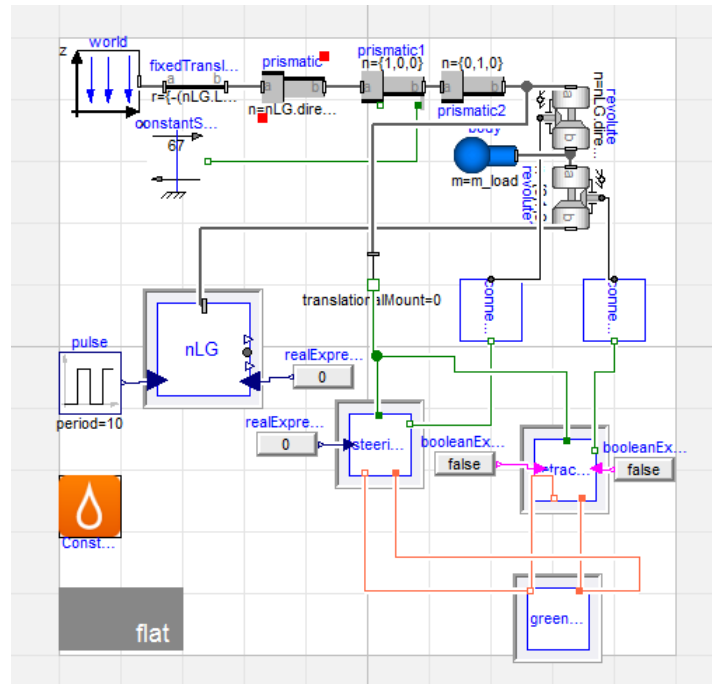


Figure 3.5: Test rig

3.5 Parametrization

In this thesis, the parametrization is confidential information so that there will be no exact value for the parameters used except for the public ones. Some of the confidential parameters such as torsion link spring-damping constants are set to experienced value so that the simulation result will have more general performance. The linear tyre model are modified according to the math model but impossible to arrange parameters of the MF-Swift model because of the limited access to it. A suitable set of parameters is selected after a large amount of trials and the whole system with Dymola tyre model is analyzed in next chapter.

4

System Analysis

4.1 Simulation

Since the MF-Swift model has been validated for vibrations in the velocity range between $7m/s$ to $40m/s$ by TASS International [7]. Only the phenomenon when V equals to the real taxiing velocity is simulated in this thesis and according to the manual, the integration step should be located between 10^{-4} and 10^{-6} . To make a comparison, the parameters used in the model with Modelon's tyres should be set similar as much as possible to MF-Swift model. The comparison is shown in figure 4.1 and 4.2.

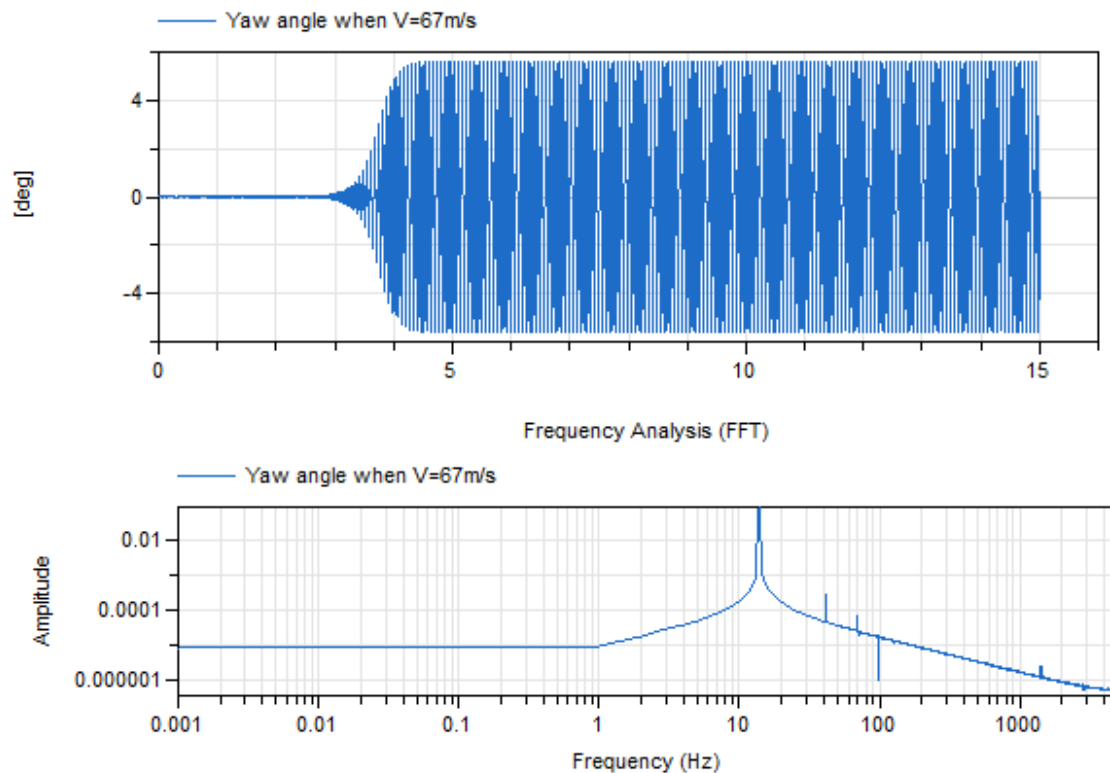


Figure 4.1: MF-Swift model simulation

4. System Analysis

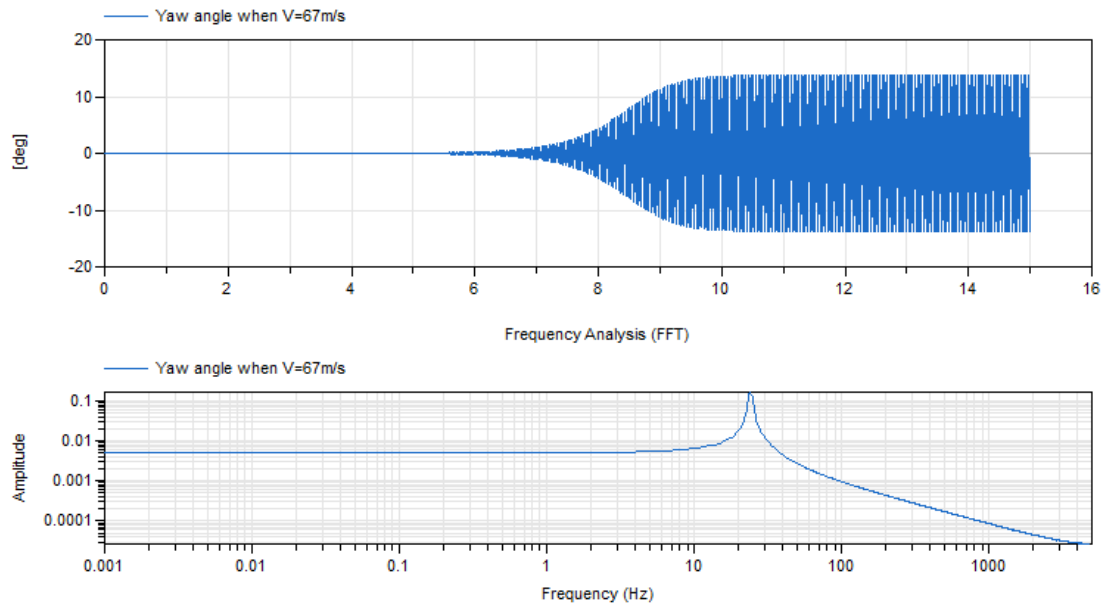


Figure 4.2: Linear tyre simulation

The MF-Swift model uses a rigid contact method to generate shimmy phenomenon and therefore, the first 2s is used to reach an equilibrium. The output has an amplitude of 6 degrees with 14Hz frequency corresponding to the normal shimmy. The Modelon's tyre model is parametrized with theoretical values and tested at the same testing velocity, the amplitude is about 15 degrees and the frequency is 24Hz. The result comparison shows that for the modified linear tyre model, it has correct shimmy features for analysis and to make a full velocity range analysis, the linear model is simulated in low ($V = 20m/s$), medium ($V = 67m/s$) and high ($V = 300m/s$). The shimmy curves on different velocities are shown in figure 4.3.

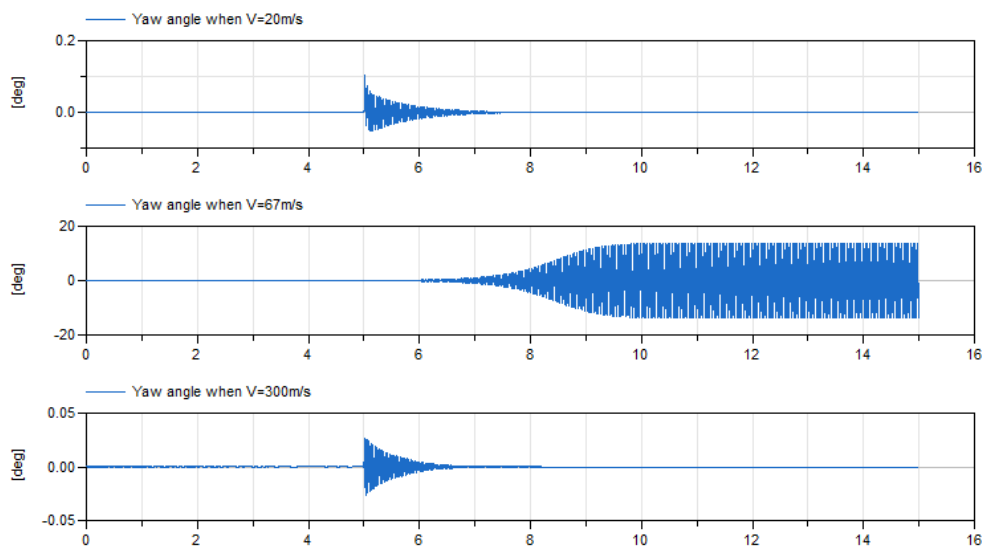


Figure 4.3: Complete Simulation result

4.2 System Analysis

The landing gear system is always a nonlinear system and to design a controller, a linear analysis including stability, controllability and observability is necessary to be taken. In Dymola, there is a Modelica LinearSystem2 library for automatic linear analysis. To have a controller for general operation, taxiing velocity and shift disturbance are considered as uncontrollable inputs and a torque applied on the torsion link joint is the controlled signal. The system is linearized at 15s when all states are steady and all inputs are 0. One limitation is that the servo valve does not have explicit transfer function and it will not be included in the linear analysis.

4.2.1 Stability

For a general system

$$\dot{x}(t) = f(x(t), t) \quad (4.1)$$

where $x(t_0) = x_0$, $x(t) \in \mathbb{R}^n$, f is a continuous mapping function and $f(\bar{x}, t_e)$ is an equilibrium.

For nonlinear system, the system is said to be Lyapunov stable if for every $\varepsilon \leq 0$, there exists a $\delta \leq 0$ such that if $\|x(t_0) - \bar{x}\| \leq \delta$, then for every $t \geq t_0$, $\|x(t) - \bar{x}\| \leq \varepsilon$ [12]. If when $t \rightarrow \infty$, $\lim_{t \rightarrow \infty} \|x(t) - \bar{x}\| = 0$, the system is asymptotic stable. Same as the theoretical model, for controller design, the system should be linearized as 15s without any inputs when all states become stable. The stability is checked by 'zero-pole' graph.

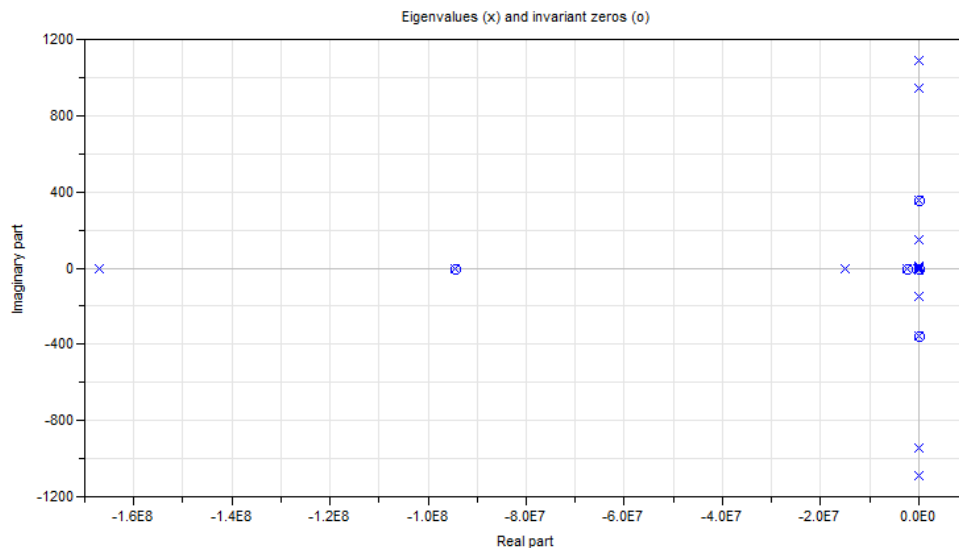


Figure 4.4: Zeros and poles of system

For the linearized system, there are some poles have very small positive real parts (about 10^{-7}) compared with other poles which means the system could be considered Lyapunov stable. Therefore, the control target is to make the system asymptotic stable.

4.2.2 Controllability and Observability

Controllability, or reachability in another word, is the ability that if a specific input signal could drive all its states to any position in its reachable configuration space. For a linear time invariant model shown in simultaneous equations 4.2.

$$\begin{aligned} \dot{x}(t) &= Ax(t) + Bu(t) \\ y(t) &= Cx(t) \end{aligned} \quad (4.2)$$

The controllability could be checked by a reachability matrix:

$$O = [B \quad AB \quad A^2B \quad \dots \quad A^{n-1}B] \quad (4.3)$$

If R is full rank, then the system is controllable [14].

Observability is the ability that if all states of the system could be decided by specific inputs and its output response. The observability is verified by the observability matrix:

$$W = \begin{bmatrix} C \\ CA \\ C^2A \\ \vdots \\ C^{n-1}A \end{bmatrix} \quad (4.4)$$

In Dymola, the controllability and observability are invested controllable but not observable using linear analysis function. In this condition, another controllability called output controllability is introduced for output control. Output controllability describes if a specific sequence of inputs could govern all outputs to any reachable states. Then the system is necessary to be simplified.

4.3 Simplification

To apply output control strategy, the outputs should be transferred to states without additional effects on the system. Then new states vector $\tilde{x}(t) = y(t) = Cx(t)$. Therefore, the simplified model is reformulated as 4.5

$$\begin{aligned} \dot{\tilde{x}}(t) &= \tilde{A}\tilde{x}(t) + \tilde{B}u(t) \\ y(t) &= \tilde{x}(t) \end{aligned} \quad (4.5)$$

where $\tilde{A} = CAC^{-1}$, $\tilde{B} = CB$. For the reason that C is a column vector, it is impossible to invert C directly and the operation pseudo-inverse is applied. The original and simplified systems are compared in the bode diagram shown in figure 4.5. Both the simplified system and the original system have similar dynamic characters in the frequency domain. This bode graph illustrates that

- The reformulation does not change the stability of system (both magnitude margin and phase margin are positive).
- The original system has a peak at high frequency domain while the simplified system does not have. But since the shimmy frequency is between 0 to 100Hz which is much lower than the peak frequency, this difference will not affect the shimmy dynamics.

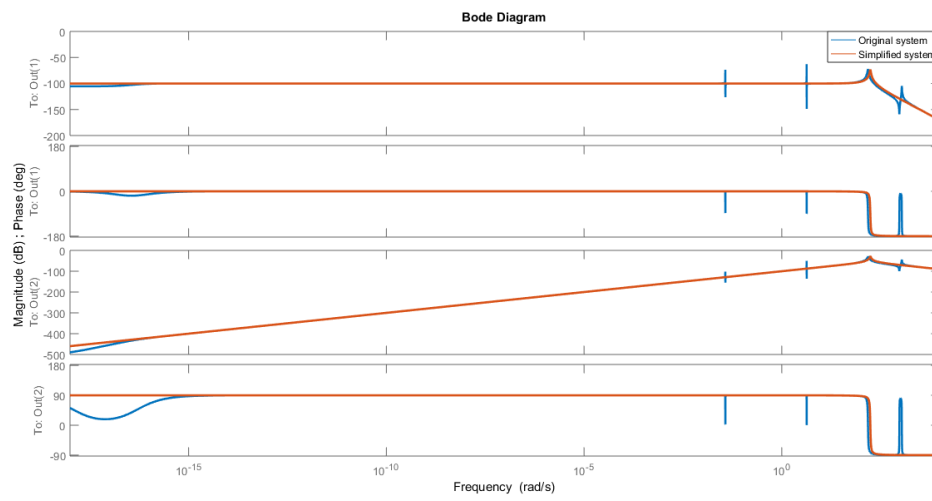


Figure 4.5: Bode diagram

5

Controller Design

The control target is to make the system asymptotic stable. A possible advanced method is to use model predictive control which is widely accepted by modern control systems. It calculates the first optimized controlled input depending on a finite horizontal window of set points with known outputs and estimated outputs iteratively. The main benefit is that current state is optimized by taking limit future states into account [13]. For the model used in this thesis, MPC is not a suitable method because there is no sufficient method to update the system state space model at every sampling interval. Another control algorithm is infinite LQR which could minimize a cost function related to states offset and input energy. In this chapter, a Linear quadratic regulator is designed and a PID is applied as a contrast experiment.

5.1 PID Control

PID control is a control algorithm that minimize the error $\epsilon(t) = r(t) - y(t)$ where $r(t)$ is the reference or set-points and $y(t)$ is the measured output. Usually, the controller is composed of the proportional, integral and differential processes while some of these factor could be 0. The control algorithm is shown below.

$$u = k_p(\epsilon(t) + \frac{1}{T_i} \int_0^t \epsilon(t)dt + T_d \frac{d\epsilon(t)}{dt}) \quad (5.1)$$

The PID control strategy could be described in detail as followed:

- Proportional action controls the current error by a proportional gain k_p . It decreases steady error but it is impossible to eliminate it because the controlled output is proportional to the offset between set points and measured outputs. Meanwhile a very high proportional gain makes system unstable while in contrast, smaller proportional gain does not have enough control effects.
- Integral action depends on an integral time constant T_i and the accumulation of past error. It is possible to remove steady offset but as a drawback, it will generate overshoots at the same time.
- Differential action works by minimizing the error derivative with a derivative time constant T_d . It enhances the system stability, reduces overshoots and improves transient performance.

5. Controller Design

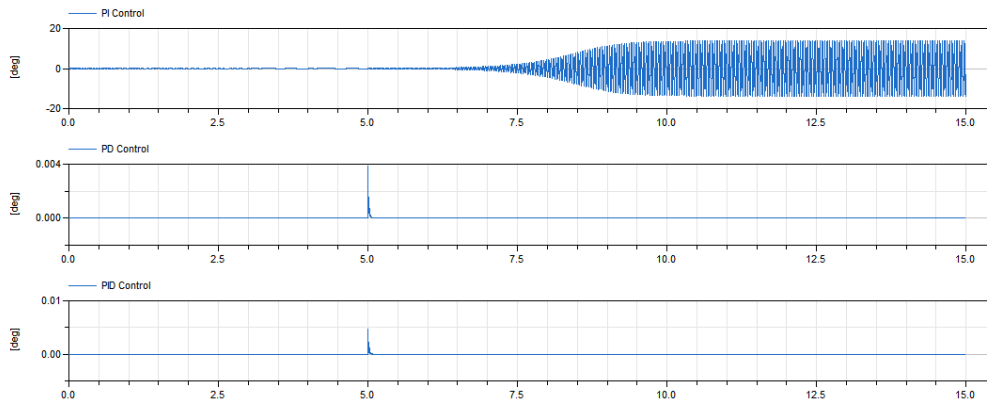


Figure 5.1: Yaw angle using PI, PD, PID controllers

In Matlab, the control toolbox could automatically tune the parameters. PI, PD and PID controlled responses are shown in figure 5.1.

The PI controller cannot reduce shimmy while PD and PID controller are effective to remove shimmy with similar responses. The setting times of them are all less than $0.1s$ and PID has better performance. In figure 5.2, the bode graph shows that the PID controller amplifies the magnitude of the error to enhance the regulating effects. But meanwhile, it generates a disturbance in high frequency. Since low frequency disturbances could be removed together with shimmy by the controller, a compensator is activated to remove high frequency disturbance. It is clear that the PID controller generates about 90 -degree offset after about $200rad/s$ in phase graph which is suitable for a first order low pass filter with a cut-off frequency higher than $200Hz$. With the transient behavior of the low pass filter considered, the low pass filter is formulated as 5.2

$$C = \frac{1}{1 + \frac{1}{400}s} \quad (5.2)$$

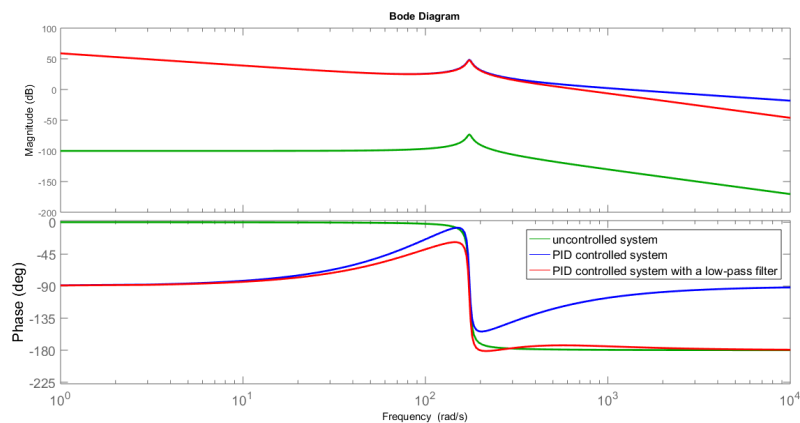


Figure 5.2: Bode graph of uncontrolled system, PID controlled system and PID controlled system with low-pass filter

5.2 LQR Design

The LQR process refers to [14]. For a given controllable and observable linear system:

$$\dot{x}(t) = Ax(t) + Bu(t) \quad (5.3)$$

A cost function

$$J = \int_0^{\infty} x(t)^T Q x(t) + u(t)^T R u(t) dt \quad (5.4)$$

is formulated for an optimal controller design. Q and R are weight matrices designed by engineers. They should fulfil the requirements that Q is positive definite or positive semi-definite symmetry matrix and R is positive definite symmetry matrix. The selection of Q and R depends on the exact requirements for systems. The control target is to minimize J over an infinite window and choose the closed-loop poles accordingly. Formally, $J^* = \min_{u(t)} J$ subjects to the system dynamics and boundary conditions with the input $u(t)$.

To solve this optimal problem, an Lagrange fomula is formulated as equation 5.5

$$L = x^T Q x + u^T u + \lambda(Ax + Bu - \dot{x}) \quad (5.5)$$

where x refers to $x(t)$, u refers to $u(t)$ and λ is the Lagrange variable or co-state. The Euler-Lagrange equations are expressed according to the rule $\frac{\partial L}{\partial \star} - \frac{d}{dt} \frac{\partial L}{\partial \dot{\star}} = 0$ where \star means optimal.

$$\begin{aligned} \frac{\partial L}{\partial u} - \frac{d}{dt} \frac{\partial L}{\partial \dot{u}} &= 0 \rightarrow u^* = -R^{-1} B^T \lambda \\ \frac{\partial L}{\partial \lambda} - \frac{d}{dt} \frac{\partial L}{\partial \dot{\lambda}} &= 0 \rightarrow \dot{x} = Ax - BR^{-1} B^T \lambda \\ \frac{\partial L}{\partial x} - \frac{d}{dt} \frac{\partial L}{\partial \dot{x}} &= 0 \rightarrow \dot{\lambda} = -Qx - A^T \lambda \end{aligned} \quad (5.6)$$

In matrix form,

$$\begin{bmatrix} \dot{x} \\ \dot{\lambda} \end{bmatrix} = \begin{bmatrix} A & -BR^{-1} B^T \\ -Q & A^T \end{bmatrix} \begin{bmatrix} x \\ \lambda \end{bmatrix} \quad (5.7)$$

and

$$u^* = R^{-1} B^T \lambda \quad (5.8)$$

Assume $\lambda^* = P(t)x(t)$ where P is a positive symmetric matrix. Then

$$\lambda^* = \dot{P}x + P\dot{x} = -Qx - A^T P x \quad (5.9)$$

Rearrange equations and apply equation 5.6 to equation 5.10

$$\dot{P} + PA - PBR^{-1} B^T P + A^T P + Q = 0 \quad (5.10)$$

For an infinite time steady situation, $\dot{P} = 0$, then Control Algebraic Riccati Equation(CARE) is introduced as equation 5.11.

$$PA - PBR^{-1} B^T P + A^T P + Q = 0 \quad (5.11)$$

The optimal controlled input is

$$u^* = -Kx = -R^{-1}B^T Px \quad (5.12)$$

For controller design, it is engineers' task to select suitable state weight matrix Q and input weight matrix R. Generally, there is no clear requirements for shimmy control but still, the controller is constrained by the actuator. Here, 'Bryson rule' is used for Q and R selection [15]. In Bryson rule,

$$Q = \begin{bmatrix} \frac{q_1}{x_{1max}^2} & & & & \\ & \frac{q_2}{x_{2max}^2} & & & \\ & & \ddots & & \\ & & & \frac{q_n}{x_{nmax}^2} & \end{bmatrix} \quad (5.13)$$

$$R = \begin{bmatrix} \frac{r_1}{u_{1max}^2} & & & & \\ & \frac{r_2}{u_{2max}^2} & & & \\ & & \ddots & & \\ & & & \frac{r_m}{u_{mmax}^2} & \end{bmatrix} \quad (5.14)$$

The x_{imax} and u_{jmax} are the boundary limitations of the inputs and outputs while $q_{1,2,...,n}$ and $r_{1,2,...,m}$ are design parameters for engineers. In this thesis, Q is designed as identical matrix with different ratio from 1 to 10^5 . Without controlled input constraint, R keeps as a constant 1. The simulation result shown in figure 5.3 expresses that from $q_i = 1000$, the controller could stabilize the yaw angle and yaw angle velocity and the offset keeps at a low level when $q_i = 10^5$.

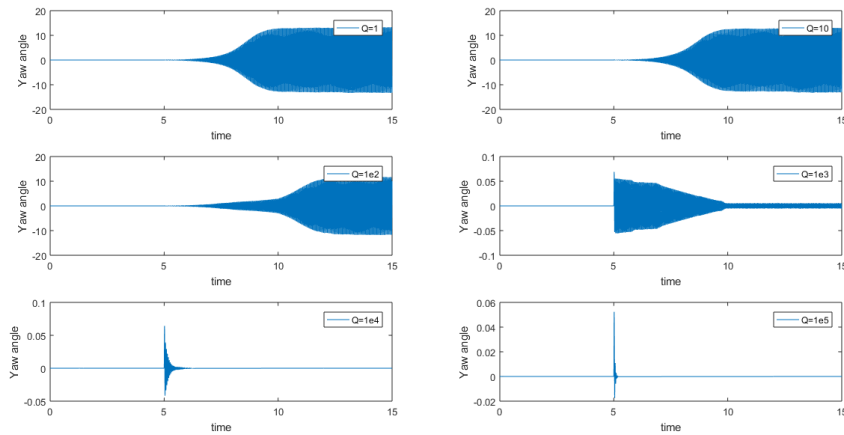


Figure 5.3: Simulation results with different Q

5.3 Controller Analysis

In this section, the dynamic character of the closed loop system with different controllers and the open loop system are discussed. Figure 5.4 shows the controlled angle and torque of PID controlled system and LQR controlled system.

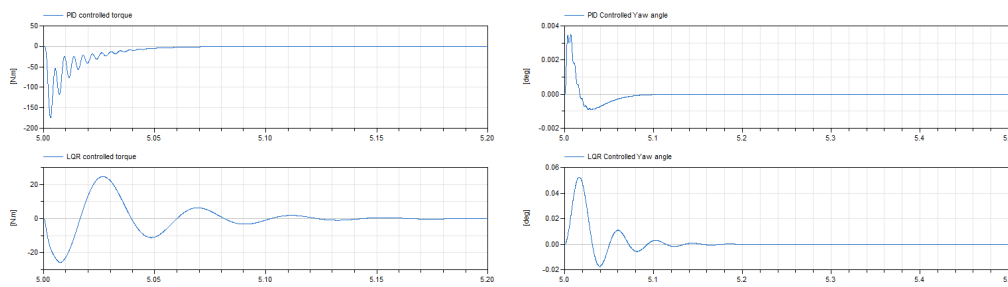


Figure 5.4: PID and LQR simulation comparison

For output analysis, PID controller designed here has better fast response character and it minimizes the amplitude more sufficiently with smaller overshoots. Based on the controlled input torque, PID needs larger torque as controlled input which will increase the size and weight of the actuator. Therefore, for aircraft production, it is better to apply LQR control algorithm to make it easily to fulfil the geometry requirements. Figure 5.5 shows the dynamic comparison of open-loop and two closed-loop systems.

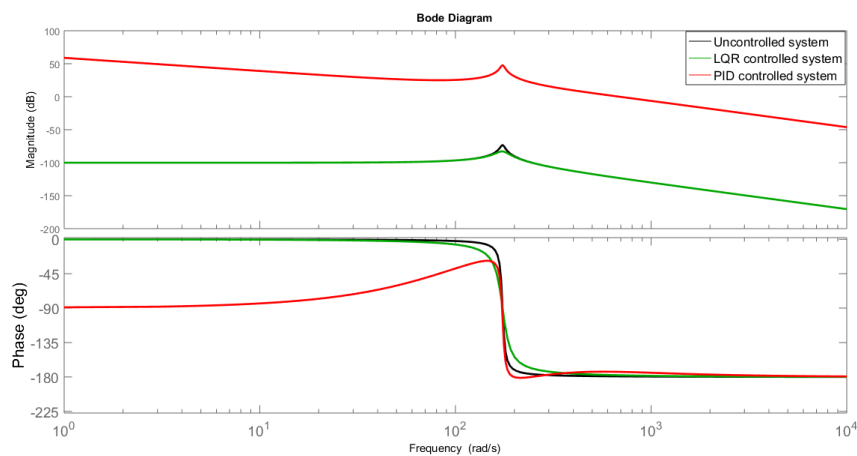


Figure 5.5: Bode graph of Open-loop, LQR controlled and PID controlled system

The bode graph both make the system stable but the reason is different.

- LQR controller minimizes the peak of the ordinary system and that increases its robustness.
- PID controller amplifies DC gain of the system and increases the attenuation speed which changes the magnitude margin and phase margin to a stable value.

6

Conclusion and Discussion

6.1 Conclusion

This report covers the whole scope from theoretical modelling to controller design. In this thesis, a Jacobian linearization method is used for nonlinear system analysis and a physical model of landing gear is proposed together with its actuating hydraulic system in Dymola. The existing tyre is optimized to generate a reasonable and suitable shimmy for aircraft taxiing dynamic analysis. An linear quadratic regulator is modified by Bryson rule successfully for shimmy control and a PID controller acts as a comparison experiment. The system analysis simplification progress could be used for controller design of the systems without all states observable.

6.2 Limitations

This thesis has the limitations and defects listed as below

- The control algorithm has to be applied by an extra actuator because it is impossible to generate the servo valve transfer function.
- The MF-Swift model is not fully accessible in this thesis which means not all parameters could be modified for Modelon's tyre component.
- There is no very sufficient method to find a steady state in Dymola except for waiting for enough time. There will be small deviations between ideal steady states and the states found.
- The test rig only simulates the airplane as a mass point with an inertia and only longitudinal, lateral, vertical movements and yaw rotation are allowed. So it still needs to be perfected.

6.3 Future Work

The landing gear model describing shimmy characters and control is able to eliminate shimmy, but still, further work listed below should be done.

- The shock absorber used in the system is a simple spring damping component but the real ones used on airplanes have more complicated dynamic characters. A complicated shock absorber model is necessary for more realistic performance.

6. Conclusion and Discussion

- Due to the limited access to tyre data and landing gear design draft, some parts of the model still need to be re-built in detail.
- An airplane body is still necessary in landing gear operation tests for better shimmy analysis and research.

Bibliography

- [1] I.J.M. Besselink. (2000). Shimmy of Aircraft Main Landing Gears(published doctoral thesis). Technische Universiteit Delft. Delft. Netherlands.
- [2] Jocelyn I. Pritchard. (1999). An Overview of Landing Gear Dynamics(NASA/TM-1999-209143). Hampton. Virginia: Langley Research Center.
- [3] Editorial staff. (1994) Landing gear topped list of aircraft systems involved in accidents during 35-year period. Flight Safety Foundation. Flight Safety Digest.
- [4] Joseph J.Destifano. Allen R.Stubberud, Ivan J.Williams. (1990) Schaum's outline of theory and problems of feedback and control systems. New York : McGraw-Hill.
- [5] Rames C. Panda. (2012) Introduction to PID Controllers - Theory, Tuning and Application to Frontier Areas. Rijeka: InTech.
- [6] Karl Johan Åström, Richard M. Murray. (2009) Feedback Systems. Princeton, New Jersey: Princeton University Press.
- [7] TASS International. (2010) Delft tyre: MF-Tyre/MF-Swift 6.1.2 Help Manual. Helmond, The Netherland. TASS International.
- [8] J.W.L.H. Maas. (2009) A Comparison of Dynamic Tyre Models for Vehicle Shimmy Stability Analysis. Eindhoven University of Technology. Eindhoven. Netherlands.
- [9] Somieski. G. (1997) Shimmy Analysis of a Simple Aircraft Nose Landing Gear Model Using Different Mathematical Methods. Aerospace Science and Technology. 87. pp545-555.
- [10] ShunHong Long. (2007) Active Control of Shimmy Oscillation in Aircraft Landing Gear(published master thesis). Concordia University. Montreal. Quebec. Canada.
- [11] H.B Pacejka. (2002) Tire and Vehicle dynamics. Oxford: Butterworth-Heinemann.
- [12] Huibert. Kwakernaak, Paphael.Sivan. (1972) Linear Optimal Control Systems. New York: Wiley. cop.

- [13] Basil Kouvaritakis, Mark Cannon. (2015) Model Predictive Control Classical, Robust and Stochastic. Oxford: University of Oxford.
- [14] Balázs Kulcsár. (2014) Linear Control System Design[PowerPoint slides]. Chalmers University of Technology.
- [15] Jonathan P, Prof. Emilio Frazzoli. (2010) Feedback Control Systems[PowerPoint slides]. MIT.